Progress In Electromagnetics Research Letters, Vol. 6, 165–174, 2009

DUAL-BAND AND WIDEBAND DESIGN OF A PRINTED DIPOLE ANTENNA INTEGRATED WITH DUAL-BAND BALUN

X. Li, L. Yang, S.-X. Gong, and Y.-J. Yang

National Key Laboratory of Antennas and Microwave Technology
Xidian University
Xi'an, Shaanxi 710071, P. R. China

Abstract—A dual-band printed dipole antenna with integrated balun feed is given in this paper. First, the fork-shaped slot is etched on the arms of the printed dipole antenna to achieve the dual-band operation with resonances at WLAN bands. The radiating element without balun is optimized and operates at 2.4 GHz (2180–2750 MHz) and 5.2 GHz (5040 MHz–5480 MHz) where return loss is less than −10 dB. In order to get a larger bandwidth, a modified Marchand balun is introduced for dual-band operation, which can provide two resonances in each band to enhance impedance bandwidth. By co-designing the radiating element with the dual-band balun, an antenna covering 2150–2750 MHz and 5050–6230 MHz bands has been achieved. The design equations for modified balun have been presented and agreement between calculation and measurement is good.

1. INTRODUCTION

In both military and commercial applications there have been an evergrowing demands for antennas that possess the following highly desirable attributes: multiband or broadband, compact size, and low profile. To fulfill the demands, a single antenna using a single feed point that covers multiband is needed. The main challenge in antenna design is to satisfy the bandwidth requirement of the various systems. Because printed microstrip antennas have been widely investigated and are attractive for their configuration advantages, printed dipole antennas are preferred in this design.

Corresponding author: X. Li (xixi1928@163.com).

In recent years there have been rapid developments in wireless local area network (WLAN) applications. WLAN can provide quick and easy wireless connection to computer, or systems in a local environment where a fixed communication infrastructure does not exist, or where such access is not permitted [1]. In order to conform to IEEE 802.11b/g and 802.11a WLAN standards, multiband antennas operating at 2.4 GHz (2412–2484 MHz), 5.2 GHz (5150–5350 MHz) and 5.8 GHz (5725–5825 MHz) frequency bands are highly desirable. Several printed antennas for WLAN applications have been reported in the literature [2–11]. A dipole antenna for WLAN 2.4/5.2 GHz is presented in [2]; measured bandwidth at the lower and upper frequency bands are 9.3 and 5.1% respectively, which are insufficient for the target in this paper. Other dual-band antennas without balun proposed in [3–5] are unsuitable for connection to a singled transceiver.

In this paper, a dual-band printed dipole antenna integrated with modified Marchand balun [12] has been presented; the balun can provide two resonances in each band to enhance impedance bandwidth. The technique used in this paper only can be seen in single-band antennas [13, 14]. Although some dual-band antennas with printed balun have been reported [2, 15], unfortunately, the effect of the balun has never been explained clearly in those papers. In this design, by co-designing the radiating element with the dual-band balun, a printed dipole antenna covering 2150–2750 MHz and 5050–6230 MHz has been achieved. In the following, the design equations of the dual-band balun have been given and there is a good agreement between calculation and measurement.

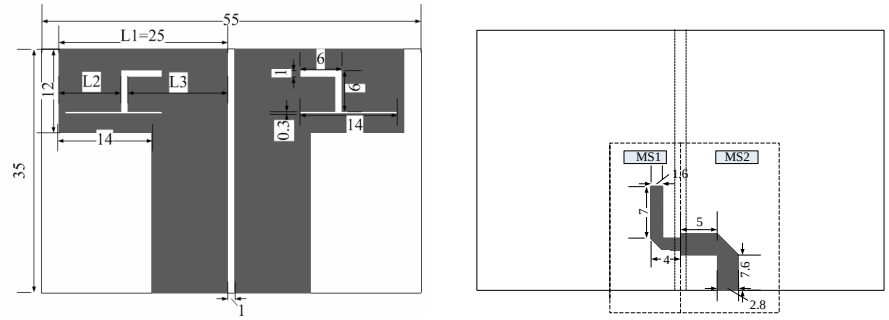

Figure 1. The configuration of the proposed antenna (a) radiating element (b) balun.

2. ANTENNA DESIGN

2.1. Radiating Element

The configuration of the radiating element is shown in Figure 1(a). The Fork-shaped slot is etched on the arms of the dipole antenna, achieving the dual-band operation with resonances at 2.4 GHz (2180–2750 MHz) and 5.2 GHz (5040–5480 MHz) (Figure 2). The overall dimensions of the structure are $55 \times 35\,\text{mm}^2$. The geometrical parameters of the radiating element are optimized using HFSS in an attempt to achieve design goals at both 2.4 and 5 GHz frequency bands.

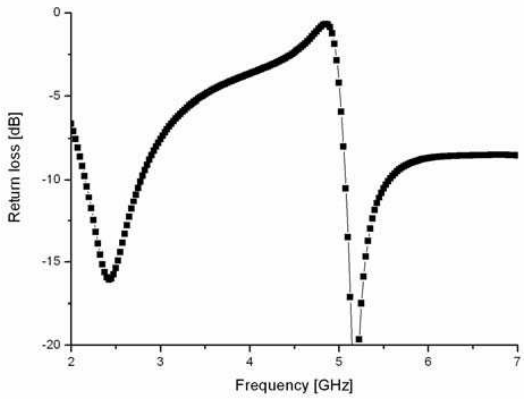

Figure 2. Simulated return loss of radiating element without balun.

At first, by carefully selecting the printed dipole arms and width, the printed dipole antenna can operate in different bands. With the presence of the fork-shaped slot, two additional dipole arms are obtained. As can be seen in Figure 3 and Figure 4, the longer path length ($L_1 + L_2$) determines the centre frequency of the lower band, whereas the shorter path length (L_3) determines the centre frequency of the higher band. The simulated input impedance of radiating element without balun can be seen in Figure 5. It should be noted that although the dipole antenna without balun has a reasonably large bandwidth, as can be seen in Figure 2, it is far from sufficient for the targeted application here.

2.2. Balun

The balun is based on Marchand balun [6], which essentially is a microstrip to co-planar strip line (CPS) transition with associated $\lambda/4$-stubs. In this design, this stub is replaced with a true open circuit. The

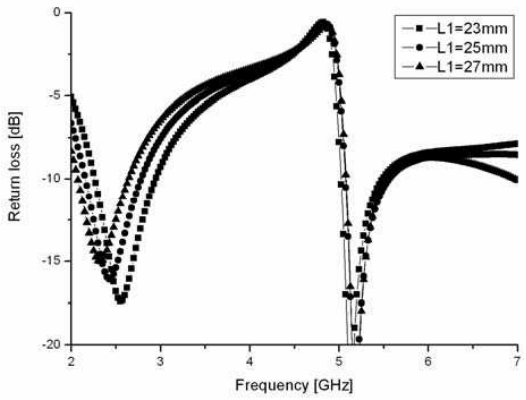

Figure 3. Simulated return loss of the radiating element for various L_1.

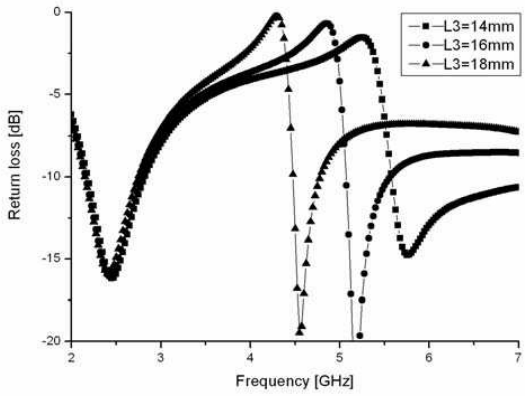

Figure 4. Simulated return loss of the radiating element for various L_3.

CPS line, with characteristic impedance $Z_{CPS} = 113\,\Omega$ and electrical length ($\beta l = 115.6°$) at 2.4 GHz, rotates the impedance of the radiating element seen in Figure 5 into the values with input resistance (R_{L+CPS}) closed to $50\,\Omega$ at both 2 and 5 GHz (Figure 6) using design equation as follows:

$$Z_{L+CPS} = Z_{CPS}\frac{Z_L + jZ_{CPS}\tan(\beta l)}{Z_{CPS} + jZ_L\tan(\beta l)} \tag{1}$$

As can be seen from Figure 6, the reactance (X_{L+CPS}) is about $j70\,\Omega$ at 2.4 GHz. At first, the open microstrip stub (MS1), with

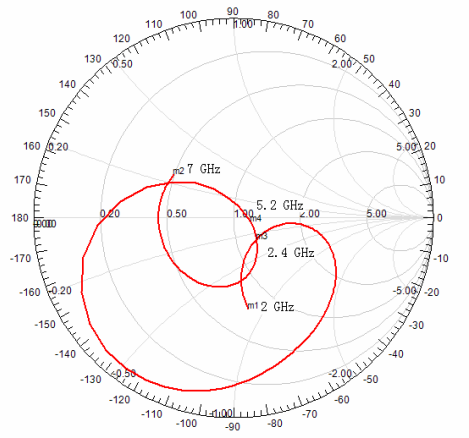

Figure 5. Simulated input impedance of radiating element (Z_L).

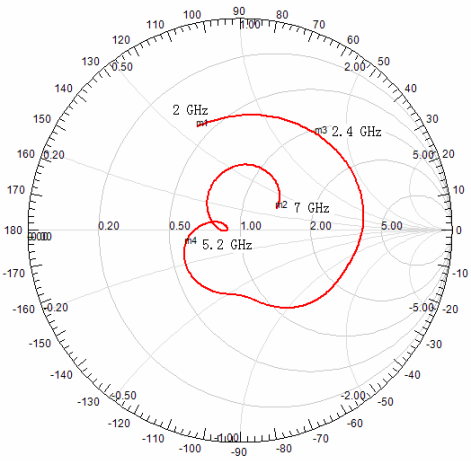

Figure 6. Simulated input impedance of radiating element and CPS line (Z_{L+CPS}).

characteristic impedance $Z_{MS1} = 70\,\Omega$ and electrical length $\beta l_{MS1} = 45^\circ$ at 2.4 GHz, adds the impedance $Z_{in,MS1} = -jZ_{MS1}\cot(\beta l_{MS1})$ to X_{L+CPS}, moving the entire band closer to $50\,\Omega$. Subsequently, at the upper frequency band, Z_{MS2} and βl_{MS2} are determined to compensate reactance according to (2)

$$Z_{in} = Z_{MS2}\frac{(Z_{in,MS1} + Z_{L+CPS}) + jZ_{MS2}\tan(\beta l_{MS2})}{Z_{MS2} + j(Z_{in,MS1} + Z_{L+CPS})\tan(\beta l_{MS2})} \tag{2}$$

Fortunately, the reactance (X_{L+CPS}) is closed to zero at the upper frequency band, so Z_{MS2} is determined as 50 Ω, and βl_{MS2} is arbitrary value. The complete balun is shown in Figure 1(b). As can be seen from Figure 7, the proposed balun can provide two resonances at 2.5 and 5.8 GHz to achieve dual-band characteristics. The simulated input impedance of complete antenna is shown in Figure 8.

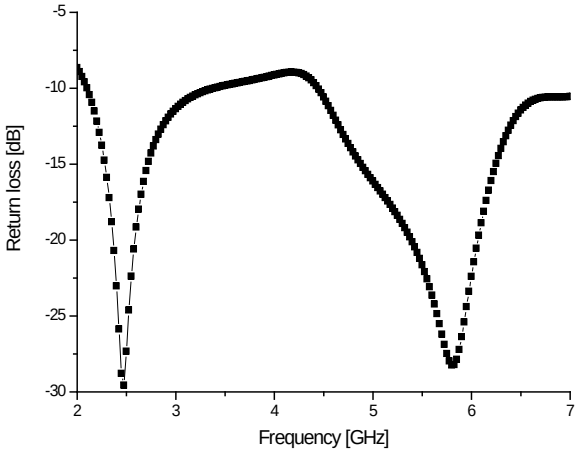

Figure 7. Simulated return loss of the proposed dual-band balun.

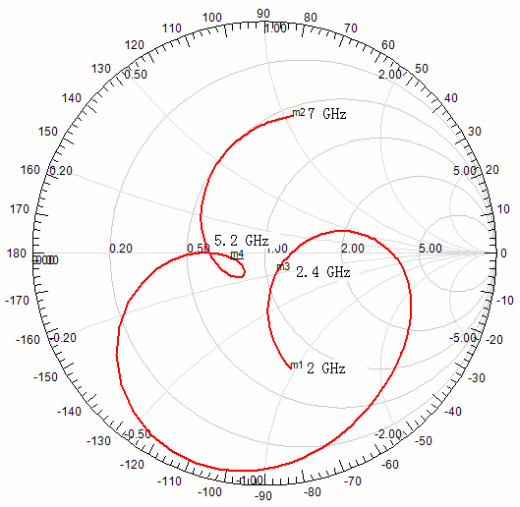

Figure 8. Simulated input impedance of complete antenna (Z_{in}).

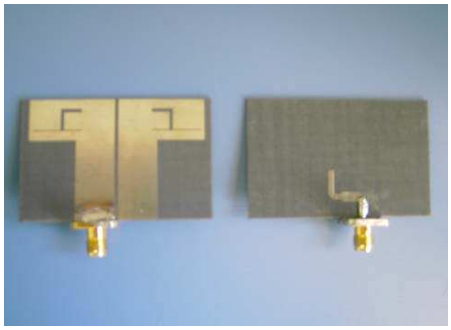

Figure 9. The photo of the proposed antenna.

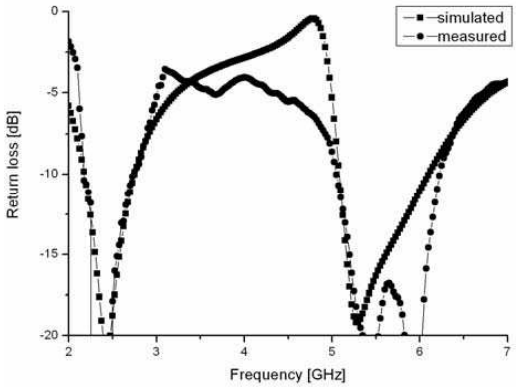

Figure 10. Simulated and measured return loss of complete antenna.

3. EXPERIMENTAL RESULTS

Figure 9 shows the prototype of the optimized printed dipole antenna, which is printed on the substrate of thickness $h = 1\,\text{mm}$ and relative permittivity $\varepsilon_r = 2.65$. Figure 10 shows the frequency response of the reflection coefficient (S_{11}) at the input port of the balun. In the lower resonant band, the measured bandwidth for $S_{11} < -10\,\text{dB}$ is about 600 MHz (2.15–2.75 GHz), which is corresponding to 24.6% of the centre frequency of 2.435 GHz. For the higher band, an impedance bandwidth of 21% (for $S_{11} < -10\,\text{dB}$), corresponding to the frequency range 5.05–6.23 GHz, was also obtained. As a result, the impedance bandwidth covers the 2.4/5.2/5.8 GHz WLAN operations. The measured far-field radiation patterns at 2.4, 5.2 and 5.8 GHz frequency bands are illustrated in Figure 11. Almost omnidirectional

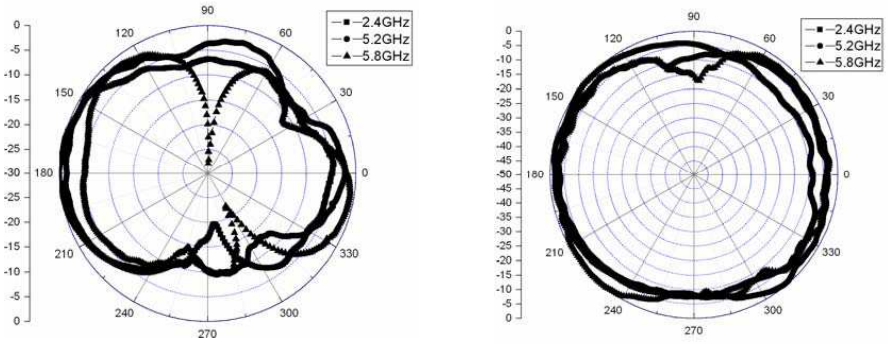

Figure 11. Measured far-field radiation patterns at 2.4, 5.2 and 5.8 GHz (a) E-plane (b) H-plane.

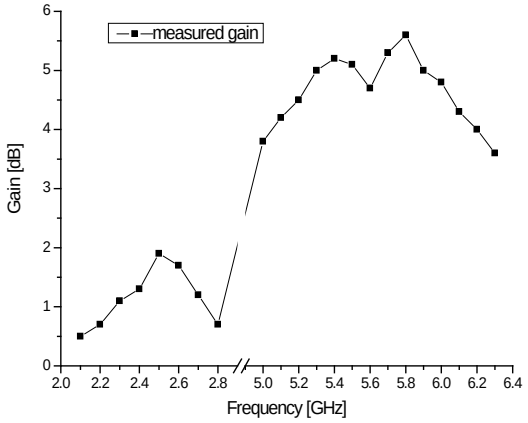

Figure 12. Measured peak gain of the proposed antenna.

patterns in the H-plane are observed for both operation frequencies. Figure 12 shows the measured peak gain of the proposed antenna. The measured gain varies from 0.5–1.9 dB across the frequency band from 2.1–2.8 GHz, and 3.6–5.6 dB across the frequency band from 5–6.3 GHz.

4. CONCLUSIONS

A novel wide- and dual-band printed dipole antenna for WLAN operations has been proposed in this paper. By using a modified Marchand balun for dual-band operation, two resonances are obtained

in each band, giving a wide impedance bandwidth. Detailed depiction of the radiating element and the effect of the balun have been presented. The concept is easily extended to other frequency band applications.

REFERENCES

1. Prommak, C., J. Kabara, D. Tipper, and C. Charnsripinyo, "Next-genner-ation wireless LAN system design," *Proc. MILCOM*, Vol. 1, 473–477, 2002.
2. Chen, H. M., J. M. Chen, P. S. Cheng, and Y. F. Lin, "Feed for dual-band printed dipole antenna," *Electron. Lett.*, Vol. 40, 1320–1322, 2004.
3. Suh, S. Y., A. E. Waltho, L. Krishnamurthy, D. Souza, S. Gupta, H. K. Pan, and V. K. Nair, "A miniaturized dual-band dipole antenna with a modified meander line for laptop computer application in 2.5 and 5.5 GHz WLAN band," *IEEE Antennas and Propagation Society Int. Symt.*, 2617–2620, 2006.
4. Zhang, Z., M. F. Iskander, J. C. Langer, and J. Mathews, "Dual-band WLAN dipole antenna using an internal matching circuit," *IEEE Trans. Antennas Propagat.*, Vol. 53, 1813–1818, 2005.
5. Su, S. W. and J. H. Chou, "Low cost flat metal-plate dipole antenna for 2.4/5-GHz WLAN operation," *Microw. Opt. Tech. Lett.*, Vol. 50, 1686–1687, 2008.
6. Liu, W. C., "Optimal design of dualband CPW-fed G-shaped monopole antenna for WLAN application," *Progress In Electromagnetics Research*, PIER 74, 21–38, 2007.
7. Wu, Y. J., B. H. Sun, J. F. Li, and Q. Z. Liu, "Triple-band omni-directional antenna for WLAN application," *Progress In Electromagnetics Research*, PIER 76, 477–484, 2007.
8. Wang, F. J. and J. S. Zhang, "Wide band cavity-baked patch antenna for PCS/IMI2000/2.4 GHz WLAN," *Progress In Electromagnetics Research*, PIER 74, 39–46, 2007.
9. Ren, W., "Compact dual-band slot antenna for 2.4/5 GHz WLAN applications," *Progress In Electrimagnetics Research B*, Vol. 8, 319–327, 2008.
10. Gao, J. P., X. X. Yang, J. S. Zhang, and J. X. Xiao, "A printed volcano smoke antenna for UWB and WLAN communications," *Progress In Electromagnetics Research Letters*, Vol. 4, 55–61, 2008.
11. Jolani, F., A. M. Dadgarpour, and H. R. Hassani, "Compact M-

slot folded patch antenna for WLAN," *Progress In Electromagnetics Research Letters*, Vol. 3, 35–42, 2008.

12. Trifunovic, V. and B. Jokanovic, "Review of printed Marchand and double Y baluns: Characteristics and application," *IEEE Trans. Micro. Theory Tech.*, Vol. 42, 1454–1462, 1994.
13. Edwards, B. and D. Rees, "A broadband printed dipole with integrated balun," *Micro. J.*, 339–344, 1987.
14. Scott, M., "A printed dipole for wide-scanning array application," *11th Int. Conf. on Antennas and Propagat.*, Vol. 1, 37–40, 2001.
15. Teo, P. H., K. S. Lee, Y. B. Gan, and C. K. Lee, "Development of bow-tie antenna with an orthogonal feed," *Microw. Opt. Tech. Lett.*, Vol. 35, 255–257, 2002.